Arab J Sci Eng (2016) 41:4065–4076
DOI 10.1007/s13369-016-2095-5

RESEARCH ARTICLE - CIVIL ENGINEERING

Rainfall–Runoff Modeling Using Support Vector Machine in Snow-Affected Watershed

Fatemeh Sedighi[1] · **Mehdi Vafakhah**[1] · **Mohamad Reza Javadi**[2]

Received: 9 December 2014 / Accepted: 18 February 2016 / Published online: 14 March 2016

Abstract Flood is one of the devastating natural disasters prediction of which is significantly important. Rainfall–runoff process and flooding are physical phenomena that their investigation is very difficult due to effectiveness of different parameters. Various methods have been implemented to analyze these phenomena. The aim of current study is to investigate the performance of the artificial neural network (ANN) (hyperbolic tangent and sigmoid) and support vector machine (SVM) (regression type-1 and regression type-2) models to simulate the rainfall–runoff process influenced by snow water equivalent (SWE) height in Roodak watershed, Tehran province, Iran. So, 92 MODIS images were gained from NASA website for three water years of 2003–2005. Then, snow cover areas in all images were extracted and finally SWE values were calculated. Also, the data of precipitation, temperature and discharge for the mentioned years were used for modeling. According to the results, ANN with the hyperbolic tangent function, rainfall-temperature-SWE inputs, 1-day delay and RMSE and R^2 of 0.024 and 0.77, and the model with the sigmoid transfer function, rain-temperature-SWE inputs and RMSE and R^2 of 0.026 and 0.75 had better prediction capability than the other models. This indicates that the SWE has improved the accuracy of the models. The results of the SVM model indicate that the model with the rainfall-temperature-SWE, 1-delay, type-1 regression, RBF function and RMSE and R^2 of 0.054 and 0.030 had better prediction capability than other models. This also shows that consideration of the SWE enhances the performance and accuracy of the SVM models. Moreover, comparing the results of ANN and SVM models, it can be concluded that ANN model with the rainfall-temperature-SWE inputs, 1-day delay, and the hyperbolic tangent function had better predictions.

Keywords Rainfall–runoff modeling · SVM · SWE · MODIS satellite · Snow cover area

✉ Mehdi Vafakhah
vafakhah@modares.ac.ir

Fatemeh Sedighi
sadighi.fatemeh@yahoo.com

Mohamad Reza Javadi
javadi.desert@gmail.com

[1] Department of Watershed Management Engineering, Faculty of Natural Resources, Tarbiat Modares University, Tehran, Iran

[2] Department of Natural Resources, Nour Branch, Islamic Azad University, Nour, Iran

1 Introduction

In the most of semiarid and arid regions of the world including Iran, the snow stored in snow pits during cold season provides a significant water resource, called snow water equivalent (SWE) in mountainous parts of the catchment [1]. This water resource plays an important role in providing basic discharge of permanent rivers and sometimes in controlling upstream flood regime of the rivers. According to the past researches, about 60 % of superficial waters and 57 % of groundwater in Iran are fed by melting snow [2]. Roodak watershed is one of the most important watersheds in the Tehran, and a considerable portion of the water requirements of its inhabitants is relied upon this watershed [3].

Snow is one of most important precipitation forms in the Latian Dam's watershed and the runoff resulted from melting snow is the main resource to feed groundwater tables because of its dilatory role and in some cases, leads to devastating floods with currents more than river capacity. Therefore, runoff estimation in a watershed is one of the basic and initial

needs in the water resource management and planning in any area.

Many models with different levels of complexity have been innovated and developed in order to estimate runoff from climatic and physical parameters of watersheds. Generally, these models can be divided into three categories including (1) black-box or empirical models, (2) conceptual models, and (3) the models based on physical relationships [4]. Black-box models usually have a physical input and output, and therefore, are completely empirical. Conceptual models of rainfall–runoff process are based on simplifying physical relations and parameters required for rainfall–runoff modeling [5]. These models are suitable for predicting coordinates of hydrographs and making them capable of efficiently creating rainfall–runoff relationships [6]. However, such geographically different relations with diverse elements in regional and areal scales are hard to be understood, and hydrologists have tried to present developed models to overcome these problems. At present, many methods are used to model hydrologic processes and runoff, of which are physical methods specifically used to simulate and calibrate these models with different complexities [7]. These methods need complicated mathematical tools [8], a big deal of calibration data, special experience and expertise [9]. When there is no or insufficient measured data for watershed properties, a database (nonphysical) model is used in order to simulate the runoff [10]. These models can be used without any mathematical complications. Artificial neural network (ANN) is a database model which has been used for hydrology in the last decade [11–27].

Farahmand [28] and Zare Abyaneh [29] compared a temporary method using the periodic neural network (PNN) with time delay and the general periodic neural network (GRNN) in modeling rainfall–runoff process in the upper part of Wordha River, India. They found that PNN model had satisfying predications 3 h earlier. Their results also showed that PNN model with time delay is more diverse than the GRNN and can be used as a secondary practical tool to predict short-term floods. Kurtulus [30] used ANN and ANFIS to predict daily discharge of Lime watersheds and compared their abilities with each other. They included the daily data of watershed for seven years in a MATLAB code and implemented an automatic instruction to select the best calibrated models. According to the results, they concluded that both models (ANN and ANFIS) accurately predicted the daily discharge of the Lime watersheds. Moreover, they improved the performance of both models through increasing inputs from one to two and reduced the root-mean-square error (RMSE). Their results also showed that ANFIS model predicts the peak flow better than ANN model. ANFIS method had better generalization capability and to some extent, better performance than ANN model, particularly for peak discharge prediction. Vafakhah [31] simulated rainfall- runoff resulted from the melted snow by ANN and neural-fuzzy methods in the Taleghan watershed, Albroz Province, Iran. The results showed that the ANN model had better capability in predicting the flow discharge than the neural-fuzzy. They also found that involving SWE height in two stations increased the performance of the network structure and increase of the number of inputs from one to three return periods in two stations, decreased the performance of the models. Pustizadeh [32] also used the same models to predict Zaiandeh-rood River flow and found that the ANFIS model gives better results than the ANN model. The above-mentioned studies reflect the high applicability of ANN method to simulate different hydrological phenomena, while ANN method has not been fully developed to model the rainfall–runoff process, nowadays is an important study topic for water researchers.

Moreover, the support vector machine (SVM) has also gained considerable successes as a new database model. The structure of SVM model was proposed by Vapnik in the 1960s. The SVM models which are based on probability theory are a type of new class of models which have been used to classify and predict in different fields. It has also been so far proved to be capable of modeling runoff and making hydrological predictions [33–36]. Wang et al. [37] used ARMA, ANN, ANFIS, SVM and genetic programming (GP) to simulate the monthly discharge for two rivers (Lankang and Woojiang) in China. The results showed that ANFIS, GP and SVM methods had the best capabilities. Wu et al. [38] also used ARMA, ANN and SVM to predict the monthly runoff of Zhiangjiabi watershed at 1, 3, 6 and 12 months later. Their results indicated that the SVM works better than other models. Moharrampoor et al. [39] predicted the daily discharge of Ghare-soo River using the SVM model. They used discharge time series of 1989–2007 period information for the river to successfully generate an artificial flow. Furthermore, Noori et al. [40] predicted the monthly flow using the SVM based on principal components analysis (PCA). Their results showed that preprocessing the input variables of the SVM model using PCA improved the performance of the SVM model. Okkan and Serbes [41] investigated the capability of the LS-SVM model to predict the runoff discharge of Tahtaali and Goros watersheds as the main water resources in Izmir city of Turkey and compared it with ANN and other common techniques including automatic average retrograde motion and multi-linear regression models. They found that LS-SVM and ANN models successfully predicted the monthly runoff discharge series with better performance in the two studied watersheds as compared to the common statistic models. Because of using different types of normalization in the process, the LS-SVM was also found to have higher accuracy than the ANN model. Shahraiyni et al. [42] used the active learning method (ALM) as a new fuzzy modeling approach to simulate long-term daily discharge of Karoon River in Iran and compared it with optimized

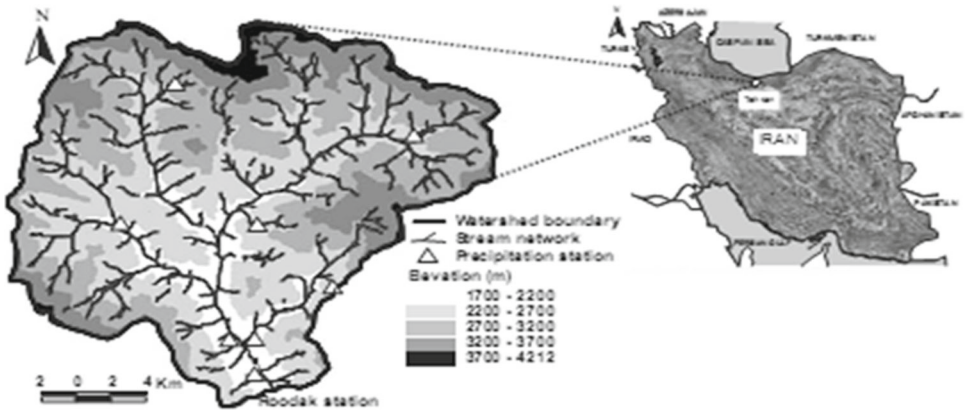

Fig. 1 Location of Roodak watershed in Iran

SVM using simple Genetic Algorithm (GA), as a well-known data-driven model. They found that the simulations could be satisfactorily applied by both ALM and optimized SVM, but working with ALM was easier than optimized SVM.

In this paper, snow-influenced Latian watershed has been studied using ANN and SVM. SWE which has not been used in researches done so far is taken into account for the first time in this paper. This consideration has led to a more accurate prediction of exiting runoff in the studied watershed.

2 Methodology

2.1 Study Area

Roodak watershed is located between longitudes (25′–51″ to 46′–51″) and latitudes (50′–35″ to 36″), with area of 436 km^2 including Garmabdar, Meigoon, Ahar, Amame, Roodak subwatersheds in Tehran. This watershed is mountainous with elevation range of 1700–4212 m above the sea level and average elevation of 2830 m. The average slope of the study area is 45.6 %, and its general slope is southward (Fig. 1).

2.2 Extracting Snow Cover Area from MODIS Images

Initially, MODIS images of the study area were downloaded from NASA website (http://ladsweb.nascom.nasa.gov) in HDF format and were imported in ENVI processor environment. Then, the satellite digital images including data preprocessing, preparation, categorization, extraction and final process were applied. Geo-referencing of the images was done automatically using the ENVI software toolbox. Atmospheric modifications were applied to the images considering the amount of wave reflexed from the Latian dam lake. It has been tried to use the images without cloud coverage on the study site. In order to provide the snow cover map, an algorithm was presented by Hall et al. [43] using bands with ground resolution of 500 m to differentiate snow from cloud. The algorithm employed to prepare the snow cover map is based on the fact that snow has high reflection in the visible wavelengths (05–0.7 μm) and has low reflection in short infrared wavelengths (1–4 μm) [43]. The bands 4 and 6 were used to automatically extract and calculate normalized difference snow index (NDSI) based on Eq. (1) as follows:

$$\mathrm{NDSI} = \frac{\mathrm{MODIS}_{\mathrm{band\,4}} - \mathrm{MODIS}_{\mathrm{Band\,6}}}{\mathrm{MODIS}_{\mathrm{Band\,4}} + \mathrm{MODIS}_{\mathrm{Band\,6}}} \quad (1)$$

where NDSI is the normalized difference snow index, $\mathrm{MODIS}_{\mathrm{Band4}}$ is MODIS 4-band image after radiometric modifications and $\mathrm{MODIS}_{\mathrm{Band6}}$ is MODIS 6-band image after radiometric modifications. This index could be used to differentiate snow from ice, also snow from clouds of above atmosphere such as cumulonimbus clouds. In fact, this index is a criterion to calculate the relative amount of differential properties which are achieved from the snow reflections between visible and infrared bands with short wavelength. The mentioned index is insensitive to exposure conditions and could be adjustable relative to the atmospheric effects. In other words, this index is dependent on not only the reflection amounts in a specific band only, but also on the digital value of reflections from the pixels. Hall et al. [43] proved that the algorithm acts the best to prepare the snow map of places with sparse vegetation such as meadows, farms and tundra. In these cases, band-2 of the MODIS would be basically processed to differentiate the snow and NDSI components of the snow map in the algorithm will effectively filter the clouds (except the high-elevation clouds). These clouds contain ice pieces and may cause to incorrect categorization of snow cover. According to this criterion, the results of NDSI index could be accepted only if the amount of reflection from band-2 would be more than 11 %. The second criterion called dark targets has been discussed by Hall et al. [44]. In this case, a 10 % reflection in band-4 is known as the lower bound for differentiation of the vegetation cover from snow. For the pixels categorized as snow, the reflection in band-4 should be more than or equal to 10 %. Despite the high value of the NDSI index, in some cases, the dark tar-

gets impede a correct categorization. Therefore, according to the two above-mentioned criteria, the snow cover algorithm would be considered a pixel as snow only if the following conditions would be satisfied:

1) Band-2 has a reflection of more than 11 %.
2) Band-4 has a reflection of more than or equal to 10 %.
3) NDSI amount should be totally estimated more than 0.4.

It should be noted that final snow map is in binary format and follows Boolean logic and in this model, the image as a whole is divided into two areas (snow and no snow).

2.3 Estimating Snow Cover Area in the Days with No Satellite Images

Having extracted the snow coverage area in different times by means of MODIS images, snow cover area in days without any images was obtained using the cumulative snowmelt depth (ΔM). ΔM is a function of degree-day factor (α) and number of the degree-days over the critical degree-day (T+) and is obtained between t_1 and t_2 from Eq. (2):

$$\Delta M\,(t_1, t_2) = \sum_{t_1}^{t_2} \left(aT^4\right) \quad t_1 < t_x \tag{2}$$

$$\alpha = 1.1\frac{\rho_\mathrm{s}}{\rho_\mathrm{w}} \tag{3}$$

where ρ_s is the snow density, ρ_w is the water density and if new snowfall occurs, the degree-day factor would be modified and introduced to the model. Assume that there are two satellite images in t_1 and t_2 and snow-covered areas extracted from these two images are SCA(t_1) and SCA(t_2), respectively. When the temperature values drop below the threshold value for melt (between t_A and t_E), snowmelt stops and the snow-covered area in t_x will be obtained from Eq. (4):

$$\mathrm{SCA}(t_x) = \mathrm{SCA}(t_{x-1}) - \frac{\mathrm{SCA}(t_1) - \mathrm{SCA}(t_2)}{\Delta M(t_1, t_\mathrm{A}) + \Delta M(t_\mathrm{E}, t_2)} \Delta M(t_{x-1}, t_x) \tag{4}$$

where SCA(t_x) indicates snow cover area in time t_x; SCA(t_{x-1}) is snow cover area in time t_{x-1}; SCA(t_1) is snow cover area in time t_1; SCA(t_2) represents snow cover area in time t_2; $\Delta M(t_1, t_\mathrm{A})$ is cumulative snowmelt depth between t_1 and t_A; $\Delta M(t_\mathrm{g}, t_2)$ represents cumulative snowmelt depth between t_g and t_2; and $\Delta M(t_{x-1}, t_x)$ is cumulative snowmelt depth between t_{x-1} and t_x.

2.4 Snow Water Equivalent (SWE)

SWE data for the Amameh snow survey station (station no: 41-007, 51 °36′E, 35 °54′N, elevation: 2350 m a.sl.) were obtained from Iranian Water Research Institute (WRI) for years of 2003–2005. In order to determine the SWE height in the days without snow survey, a linear regression relationship between the SWE and the snow cover area was used.

Table 1 The partial auto-correlation functions of the daily rainfall, temperature and SWE time series of from lag-1(r1) to lag-5(r5)

Lag	$r1$	$r2$	$r3$	$r4$	$r5$
Rainfall (mm)	0.41	−0.04	0.08	0.014	0.011
Temperature (°C)	0.98	0.12	0.07	0.025	0.028
SWE (mm)	0.98	−0.05	−0.02	−0.02	−0.01

2.5 Meteorological and Streamflow Data

Precipitation data of weather stations [Roodak, Amameh, Galookan (Kamarkhani), Rahat Abad, Ahar, Garmabdar, Shemshak, Roodbar Ghasran], the daily temperature of stations (Amame, Rahat Abad, Galookan) and the daily flow in Roodak hydrometry station were obtained from Iran Water Resources Management Company (IWRM) for the years of 2003–2005. In order to determine the average daily precipitation and the watershed temperature, Thiessen polygon used.

2.6 Data Classification

In this study, the data of average daily precipitation (P/mm), average daily temperature (t/°C), the daily SWE height (SWE/mm) and average daily discharge (Q/ m^3/s) all gathered over three water years of 2003–2005 in Roodak hydrometry station. Totally 1096 data points were used from this station. 70 % (768) of data points were used as the training set and the remaining (30 %, 330) as the test points. This was also the same for the SVM model. The daily rainfall, temperature and SWE and streamflow data statistics of training, test, validation and entire data set are presented in Table 1.

2.7 Determination of Input Parameters

Data selection is the first step in creating the neural network appropriate to estimate the rainfall–runoff equations. Generally, two types of data could be used as the input data for the neural network, which includes statistics just related to the daily precipitation, daily temperature and SWE height. To select the input values to the network, an appropriate solution could be hydrological observations in different delay times. For this purpose, the number of delays required for modeling the input variables to the network was obtained by plotting the partial autocorrelation functions in STATISTICA software (Table 2).

As can be seen from Table 2, the partial auto-correlation functions (PACF) indicated significant correlation at lag-1 for

Table 2 The statistical characteristics of the daily rainfall, temperature and SWE and streamflow data

Variable	Data set	Number of data	Average	Standard deviation	Maximum	Minimum
Rainfall (mm)	Training	768	2.08	5.47	68.90	0
	Test	328	2.01	5.21	31.67	0
	Entire	1096	2.06	5.39	68.90	0
Temperature (°C)	Training	768	10.94	8.46	29.26	−5.45
	Test	328	11.32	9.88	26.92	−9.32
	Entire	1096	11.06	9.03	29.26	−9.32
SWE (mm)	Training	768	80.87	113	292.68	0
	Test	328	79.42	112.01	292.23	0
	Entire	1096	80.43	112.66	292.68	0
Stream flow ($m^3\ s^{-1}$)	Training	768	8.99	10.21	119	2.32
	Test	328	9.98	9.36	38.7	2.17
	Entire	1096	9.28	9.97	119	2.17

rainfall and SWE after lag-2, fell within the confidence limits. and lag-1 and lag-2 for temperature after lag-3, fell within the confidence limits. The PACF suggested incorporating daily rainfall and SWE values up to 1 day-lag and daily temperature value up to 2 day-lag in input vector to the ANN and SVM models.

2.8 Data Normalization

In order to prevent underestimation of ANN weights, its inputs need to be normalized. In this study, following equation was used:

$$N_{\mathrm{i}} = 0.8 \times \left(\frac{x_{\mathrm{i}} - x_{\min}}{x_{\max} - x_{\min}} \right) + 0.1 \tag{5}$$

where N_{i} represents the normalized value; x_{i} is the real value; $x_{\min}$ and $x_{\max}$ are the minimum and maximum values, respectively. The above equation normalizes the ANN inputs between 0.1 and 0.9.

2.9 Artificial Neural Network (ANN)

The ANN is a computational mechanism which is capable to give new information on the basis of some input information and calculations [45]. One of the common ANNs used in hydrology is the multi-layer perceptron (MLP) consisted of one input layer, one output layer, and one or more hidden layers that are not directly connected to the input data and output results. The input layer units have the task of distributing input data and output layer provides replies for output signals. The number of neurons in both layers is equal to the number of the inputs and outputs. The hidden layer (s) serves as the connection between the input and output layers. There is no specific algorithm in MLP to determine the numbers of the neurons and hidden layers. The mentioned numbers are determined by trial and error.

2.9.1 Activation Functions

As common in ANN, sigmoid function consists of logistic and tangential activation functions were used in the hidden layer and linear activation function in the output layer.

2.9.2 Training Algorithm of ANN

According to Coulibaly et al. [46] here feed-forward back propagation and early stopped training algorithms were used in current study.

2.9.3 Support Vector Machine

Recently, new tools regarding artificial intelligent (AI) called a SVM has had many applications in learning method machines [47]. An explanation of this model can be found in Kecman [48] and Kakaei Lafdani [49]. The linear regression relationship is as follows:

$$y = f(X) = \langle w.x \rangle + b \tag{6}$$

where y is a dependent, x is an independent vector and w and b are parameters of the model. The method of least squares applies to determine the parameters $\langle w.x \rangle$ by minimizing the sum of squared deviations of the data, $\sum_{i=f1}^{l} (y_i \langle w.x \rangle + b)^2$. Depending on the definition of this error function, two types of SVM models can be recognized. It can be assumed that a band is placed around the function $f(x)$ which causes training error for a point out of this band and unless the covariate variable is called ξ_i. This covariate variable is for a point in zero band and increases exponen-

Fig. 2 MLP-ANN structure

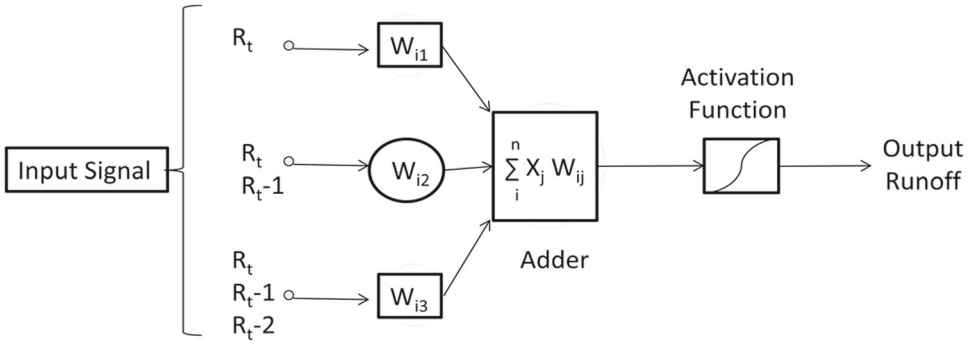

tially for outside points. This regression method is called $\varepsilon-$ SVM (regression SVM type 1) which is the most common modeling method. The cost function with ε-insensitive zones described as the following:

$$|\xi|_\varepsilon = |y - f(x)|_\varepsilon = \begin{cases} \varepsilon & \text{if } |y - f(x)| \le \varepsilon \\ |y - f(x)| - \varepsilon & \text{otherwise} \end{cases} \tag{7}$$

The aim is to determine a function $f(x)$ in a way to maximize ε-derivation. This is equivalent to minimizing the functional,

$$\text{Min}\frac{1}{2}\,||w||^2 + C\left(\sum_i^l \xi_i^* + \sum_i^l \xi_i\right) \tag{8}$$

Subject to:

$$y_i - \langle w.x\rangle - b \le \varepsilon + \xi_i \tag{9}$$

$$\langle w.x\rangle + b - y_i \le \varepsilon + \xi_i^*$$

$$\xi_i, \xi_i^* \ge 0 \tag{10}$$

where C is the cost factor and ξ_i and ξ_i^* are slack variables. An alternative form of SVM is called $\nu-$ SVM regression (regression SVM type 2). For this SVM, the error function is given by:

$$\text{Min}\frac{1}{2}w^T w + C\left(\nu\varepsilon + \frac{1}{l}\sum_{i=1}^l\left(\xi_i + \sum_i^l \xi_i^*\right)\right) \tag{11}$$

Subject to:

$$w^T\phi(x_i) + b - z_i \le \varepsilon + \xi_i \tag{12}$$

$$z_i - w^T\phi(x_i) - b \le \varepsilon + \xi_i^*$$

$$\xi_i, \xi_i^* \ge 0, \varepsilon \ge 0 \tag{13}$$

In the case of nonlinear systems, the kernel function can be used to map the data in to a higher dimensional space. Four kernel functions commonly used in regression SVM are given in Table 3.

Table 3 The different kernel functions equations

Kernel function	Formula
Linear kernel	$k(x, y) = x.y$
Polynomial kernel	$k(x, y) = [(x, y) + c]^d$
Radial basis function kernel	$k(x, y) = \exp\left(-\left\|\frac{x-y}{2\sigma^2}\right\|^2\right)$
Sigmoid kernel	$k(x, y) = \tanh(x.y + c)$

2.9.4 Network Performance Evaluation Criteria

In order to compare the results of each ANN and SVM models with observed data in the test step, to compare different networks and choose the best model, threshold values were used. The coefficient of determination (R^2) for the observed and estimated values is the most common comparison index. However, this coefficient is a general index and could not be an appropriate index [20]. Therefore, here, two more indices beside R^2 were used:

$$\text{Coefficient of determination: } R^2 = \frac{\sum_{i=1}^N \left(Q_{ci} - \bar{Q}_{oi}\right)^2}{\sum_{i=1}^N \left(Q_{oi} - \overline{Q_{oi}}\right)^2} \tag{14}$$

$$\text{Root-mean-square error : RMSE} = \sqrt{\frac{\sum_{i=1}^n (Q_{ci} - Q_{oi})^2}{n}} \tag{15}$$

$$\text{Coefficient of efficiency: CE} = 1 - \frac{\sum_{i=1}^N (Q_{ci} - Q_{oi})^2}{\sum_{i=1}^N \left(Q_{oi} - \bar{Q}_{oi}^2\right)} \tag{16}$$

3 Results and Discussion

Prediction models were obtained based on the methodology (Table 4).

As can be seen in Table 4, the SVM model with input data of the rainfall with 3-day delay, regression type-1

Table 4 Results for SVM model for both regressions (type 1 and 2) with different inputs

Model inputs	SVM type	Kernel type	RMSE		R^2	
			Train	Test	Train	Test
Rt Tt SWEt	Regression type 1	RBF	0.054	0.054	0.34	0.29
	Regression type 2	RBF	0.054	0.054	0.44	0.29
Rt SWEt	Regression type 1	RBF	0.054	0.054	0. 38	0.19
	Regression type 2	RBF	0.063	0.063	0.29	0.16
Rt Tt	Regression type 1	RBF	0.054	0.054	0.34	0.23
	Regression type 2	Polynomial	0.063	0.063	0.20	0.073
Rt	Regression type 1	Linear	0.063	0.063	0.16	0.016
	Regression type 2	Linear	0.077	0.070	0.16	0.016
Rt Rt-1Tt Tt-1 SWEt SWEt-1	Regression type 1	RBF	0.054	0.054	0.50	0.40
	Regression type 2	Polynomial	0.054	0.054	0.39	0.27
Rt Rt-1 SWEt SWEt-1	Regression type 1	RBF	0.054	0.054	0.37	0.20
	Regression type 2	RBF	0.054	0.054	0.40	0.21
Rt Rt-1Tt Tt-1	Regression type 1	RBF	0.054	0.054	0.41	0.26
	Regression type 2	RBF	0.054	0.054	0.41	0.25
Rt Rt-1	Regression type 1	Linear	0.063	0.063	0.20	0.025
	Regression type 2	Linear	0.063	0.054	0.19	0.025
Rt Rt-1Rt-2 Tt Tt-1Tt-2	Regression type 1	RBF	0.054	0.054	0.42	0.27
	Regression type 2	RBF	0.054	0.054	0.41	0.27
Rt Rt-1Rt-2	Regression type 1	Linear	0.063	0.063	0.22	0.027
	Regression type 2	Linear	0.063	0.063	0.22	0.028
Rt Rt-1 Rt-2 Rt-3 Tt Tt-1 Tt-2 Tt-3	Regression type 1	RBF	0.054	0.054	0.46	0.34
	Regression type 2	RBF	0.054	0.054	0.43	0.29
Rt Rt-1 Rt-2 Rt-3	Regression type 1	Sigmoid	0.063	0.063	0.21	0.028
	Regression type 2	Sigmoid	0.063	0.063	0.21	0.028

and sigmoid function with RMSE and R^2 of 0.063 and 0.028, respectively, and regression type-2 with sigmoid function and RMSE of 0.063 and R^2 0.028, respectively, had better performance than the model with the input rainfall with without delay and 2-day delay. Moreover, the rainfall-temperature model with 3-day delay, regression type-1, the RBF function with RMSE and R^2 of 0.054 and 0.34, respectively, and regression type-2 with the RBF function, RMSE and R^2 of 0.054 and 0.29 had better predictions compared to the rainfall-temperature models with without delay to 2-day delay. The rainfall-temperature-SWE model with 1-day delay and regression type-1 with the RBF function with RMSE and R^2 of 0.054 and 0.40 and regression type-2 with polynomial function with the RMSE and R^2 of 0.054 and 0.27, respectively, had better performance in comparison with the rainfall-temperature-SWE with no delay.

Table 5 indicates that ANN with the rainfall input with 3-day delay, hyperbolic tangent function with the 4-8-1 structure and the RMSE and R^2 of 0.054 and 0.04 had better performance than the other model with the input precipitation without and with 2-day delay. Moreover, ANN with the rainfall-temperature input and 3-day delay with the RMSE and R^2 of 0.044 and 0.32 had better performance. The model with the rainfall-temperature-SEW input, 1-day delay with the hyperbolic tangent by the 6-11-1 structure with the RMSE and R^2 of 0.024 and 0.77 had better performance than the same model with no delay; also, the ANN network with rainfall input, three days delay, sigmoid transfer function, the 4-3-1 structure and the RMSE and R^2 of 0.054 and 0.030 had better performance than the model with the rainfall input, without or with up to 2-day delay. Moreover, ANN model with the rainfall-temperature input, 3-day delay, the sigmoid transfer function of the 8-14-1 structure and with the RMSE and R^2 of 0.045 and 0.34 had better performance than the model with the rainfall-temperature input, without or with up to 2-day delay. In the model with the rainfall-temperature-SWE, 1-day delay, 6-9-1 structure, and the RMSE and R^2 of 0.026 and 0.75 showed better performance than the same model without delay. Table 6 shows the best ANN models with the hyperbolic tangent and sigmoid functions and the SVM with the regressions type-1 and -2.

It can be seen from the Figs. 3, 4, 5, 6, 7, 8 and -9 that the best tangent hyperbolic model, the best ANN model with the sigmoid function, and the SVM with the regressions type-1 and type-2 estimated the maximum observed discharge in the test stage (38.7 m^3/s) 32.90, 36.87, 15.08, and 11.26, respec-

Table 5 ANN results with hyperbolic tangent (tan) and sigmoid algorithm functions with different inputs

Model inputs	Activation function	ANN structure	Training		Test	
			R^2	RMSE	R^2	RMSE
Rt Tt SWEt	tan	3-3-1	0.56	0.04	0.70	0.094
	log	3-7-1	0.59	0.038	0.60	0.034
Rt SWEt	tan	2-4-1	0.42	0.044	0.22	0.044
	log	2-5-1	0.42	0.044	0.22	0.044
Rt Tt	tan	2-3-1	0.34	0.044	0.28	0.044
	log	2-3-1	0.31	0.044	0.29	0.044
Rt	tan	1-2-1	0.17	0.054	0.016	0.054
	log	1-3-1	0.16	0.054	0.016	0.054
Rt Rt-1 Tt Tt-1 SWEt SWEt-1	tan	6-11-1	0.67	0.031	0.77	0.024
	log	6-9-1	0.68	0.031	0.75	0.026
Rt Rt-1 SWEt SWEt-1	tan	4-7-1	0.57	0.031	0.31	0.044
	log	4-3-1	0.51	0.031	0.25	0.048
Rt Rt-1 T,T-1	tan	4-9-1	0.42	0.044	0.26	0.044
	log	4-5-1	0.39	0.044	0.28	0.044
Rt Rt-1	tan	2-5-1	0.19	0.054	0.025	0.054
	log	2-4-1	0.19	0.054	0.025	0.054
Rt Rt-1Rt-2 Tt Tt-1Tt-2	tan	6-9-1	0.53	0.031	0.31	0.044
	log	6-3-1	0.49	0.031	0.32	0.044
Rt Rt-1Rt-2	tan	3-5-1	0.36	0.044	0.028	0.054
	log	3-3-1	0.22	0.054	0.025	0.054
Rt Rt-1 Rt-2 Rt-3 Tt Tt-1 Tt-2 Tt-3	tan	8-4-1	0.59	0.031	0.32	0.044
	log	8-14-1	0.47	0.043	0.34	0.045
Rt Rt-1 Rt-2 Rt-3	tan	4-8-1	0.37	0.044	0.04	0.054
	log	4-3-1	0.17	0.054	0.030	0.054

Table 6 The best ANN model structure with hyperbolic tangent and sigmoid functions and SVM model with both regressions

Model type	Model inputs	Structure	Training		Test		
			R^2	RMSE	R^2	RMSE	CE
ANN tan	Rt Rt-1 Tt Tt-1 SWEt SWEt-1	6-11-1	0.68	0.031	0.77	0.024	0.78
ANN log	Rt Rt-1 Tt Tt-1 SWEt SWEt-1	6-9-1	0.69	0.031	0.75	0.026	0.77
SVM type1	Rt Rt-1 Tt Tt-1 SWEt SWEt-1	RBF	0.71	0.054	0.40	0.054	0.377
SVM type2	Rt Tt SWEt	RBF	0.67	0.054	0.30	0.054	0.29

tively. Therefore, ANN model with the sigmoid function had the most accurate predictions. The corresponding estimations of the second maximum observed discharge (38.1 m^3/s) were 24.57, 26.65, 17.32, and 19.17 m^3/s, respectively. These results indicated that ANN model with the sigmoid function had the most accurate prediction.

4 Conclusions

The rainfall–runoff relationship depends on climatic and physical parameters including temporal variations in precipitation, slope, height, plant cover, soil humidity, underground water and etc. This dependency on many variables makes the rainfall–runoff relationship deviate from linear form and convert it to nonlinear complicate relationship. Many physical models have so far been proposed for this relationship, but they had not high applicability due to lack of some required parameters and some simplifications. Owing to the capability of modeling complicate nonlinear relations 'without any need for a high number of parameters, ANNs and SVM have recently attracted a lot of attentions to investigate rainfall–runoff relationship. In this study, ANN, feed-forward back propagation (FFBF), ε − SVM (regression type-1) and ν − SVM (regression type-2) were applied for rainfall–runoff modeling in snow-affected watershed.

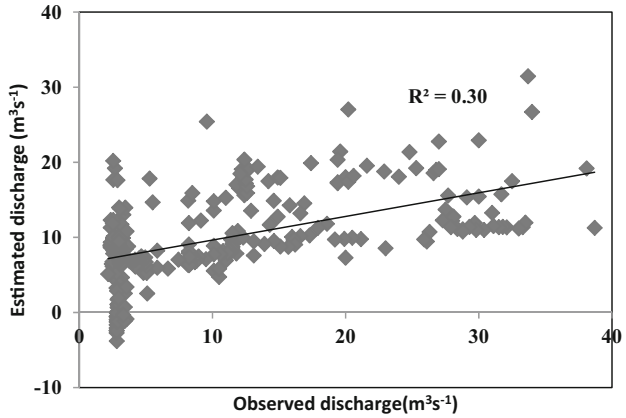

Fig. 3 Observed versus estimated discharge diagram related to type-1 SVM model with rainfall-temperature-SWE inputs, 1-day delay in test stage

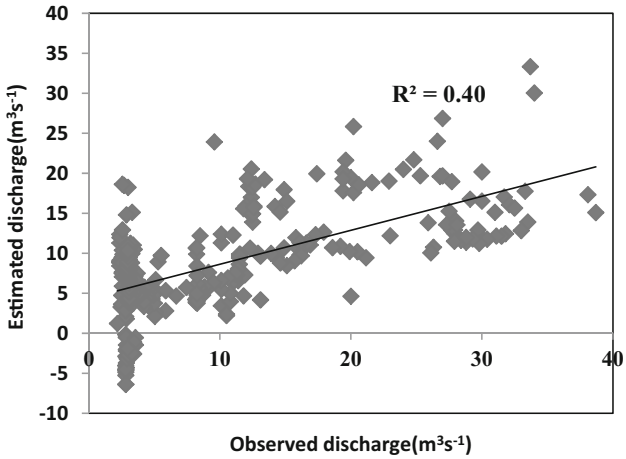

Fig. 4 Observed versus estimated discharge diagram related to type-2 SVM model with rainfall-temperature-SWE inputs, 1-day delay in test stage

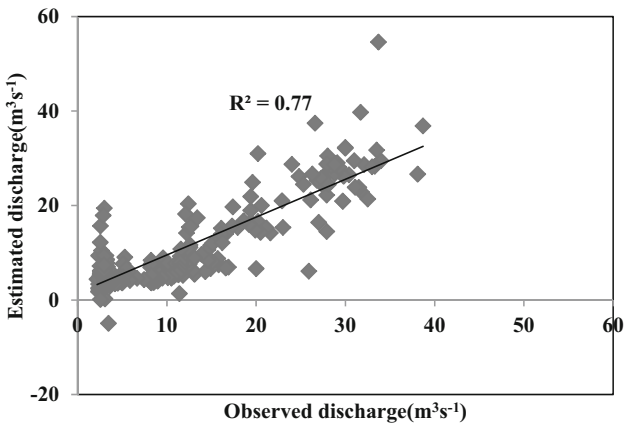

Fig. 5 Observed versus estimated discharge diagram related to ANN model with sigmoid algorithm with rainfall-temperature-SWE inputs, 1-day delay in test stage

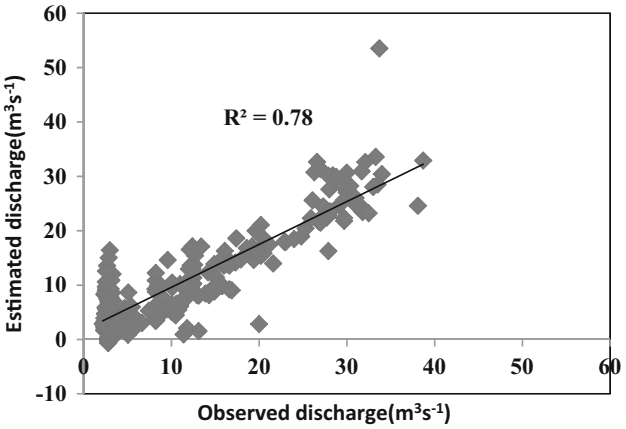

Fig. 6 Observed versus estimated discharge diagram related to ANN model with hyperbolic tangent algorithm with rainfall-temperature-SWE inputs, 1-day delay in test stage

Accordingly, SCA were obtained from 92 MODIS images for three water years of 2003–2005. Then, SWE were computed according to SCA and SWE measurements in the Amameh snow survey station. Also, the data of daily rainfall, daily temperature and daily discharge for the mentioned years were used for modeling. The results showed that the partial autocorrelation functions (PACF) values provide quite valuable information about the structure of the FFBF and SVM input layer. The examination of PACF table enables the ANN and SVM user to select the most appropriate number of input nodes preventing time losses due to the testing of several input layer alternatives. According to the results can be concluded that ANN with the rainfall-temperature input with 3-day delay, the hyperbolic tangent function and the RMSE and R^2 of 0.044 and 0.32 and ANN model with the rainfall-temperature input, 3-day delay, the sigmoid function and the RMSE of 0.045 and R^2 of 0.34 had better performance in the test step as compared with the model with the rainfall input and 3-day delay. Therefore, taking the temperature into account improved the performance of ANN and this is consistent with the findings of Lorrai [50] and Raghuwanshi et al. [51]. Moreover, ANN with the hyperbolic tangent function, the rainfall-temperature-SEW input, 1-day delay and RMSE and R^2 of 0.024 and 0.77, and the model with the sigmoid transfer function, the rainfall-temperature-SWE input and RMSE and R^2 of 0.026 and 0.75 had better prediction than other models. This indicates that consideration of the SWE improved the accuracy of the models, and this is consistent with previous results [1,13,31]. The results of the SVM model indicated that the model with the rainfall-temperature-SWE, 1-delay, regression type-1, RBF function and RMSE and R^2 of 0.054 and 0.0300, respectively showed more accurate prediction than other models implemented. This also

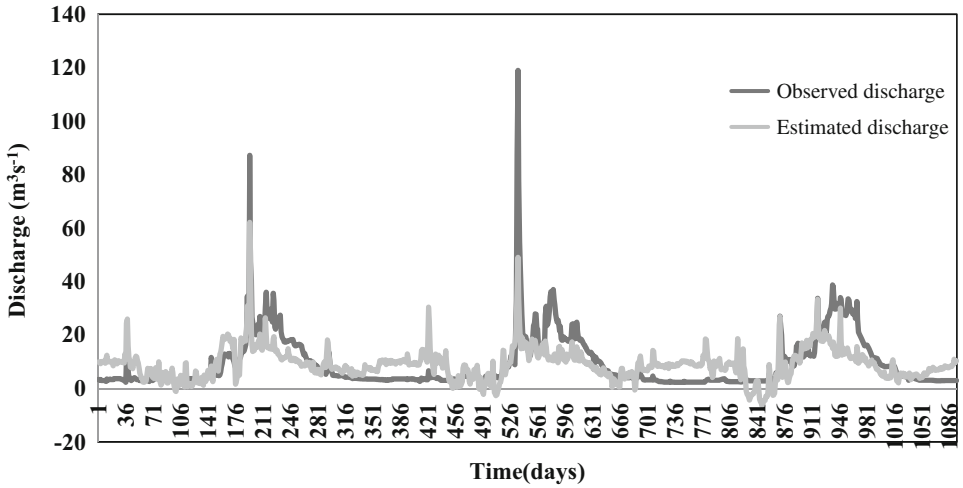

Fig. 7 Comparison of observed with estimated discharges for type-1 SVM model with rainfall-temperature-SWE inputs, 1-day delay in test stage

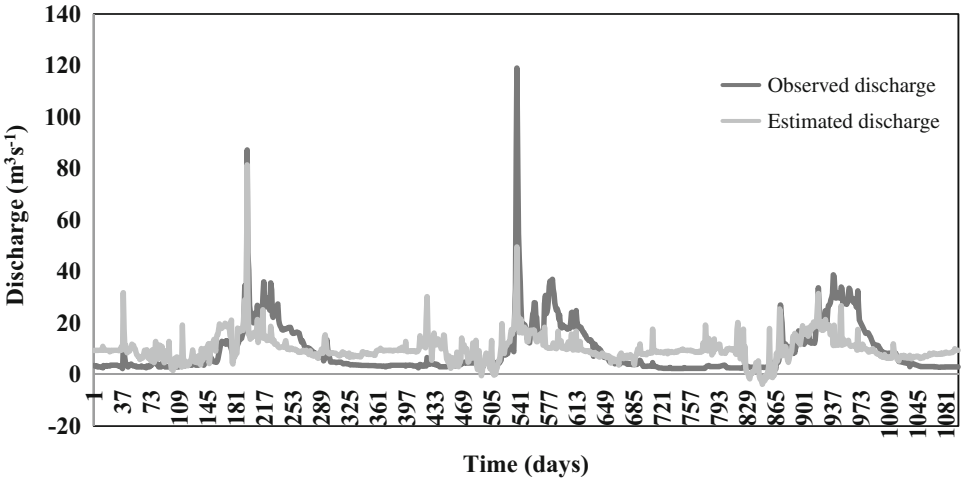

Fig. 8 Comparison of observed with estimated discharges for type-2 SVM model with rainfall-temperature-SWE inputs, 1-day delay in test stage

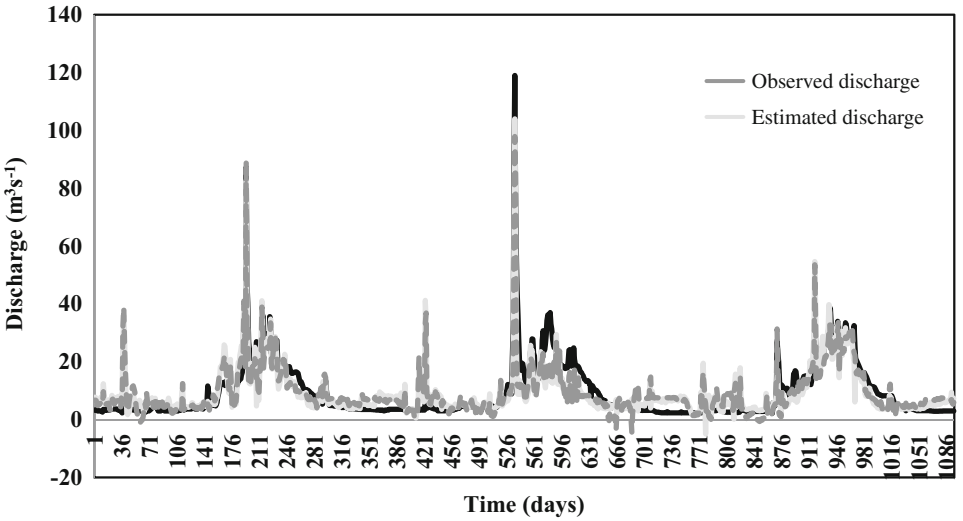

Fig. 9 Comparison of observed with estimated discharges for ANN model with rainfall-temperature-SWE inputs, 1-day delay in test stage

demonstrates that consideration of the SWE enhances the performance and accuracy of the SVM models. Moreover, comparing the results of ANN and SVM models, it can be concluded that ANN model with the rainfall-temperature-SWE input, 1-day delay, and the hyperbolic tangent function had better predictions. This result is consistent with the findings of Das et al. [52] and Muduli et al. [53]. Four parameters influence on results of the SVM models included $\gamma, C, \varepsilon - p$ and $\varepsilon - e$. However, determining the best value of the training parameters is essential. In this study, v-fold cross-validation was applied. Three years of observation data is a quite short time period for modeling. It should be noted that the results of this study are time-specific since calibration of ANN and SVM models is constrained to a specified limited length of recorded data. The models presented in this paper only applied on data from one station. Further studies using more sample data from various areas are required to strengthen these conclusions.

References

1. Tabari, H.; Maroufi, S.; Zare, H.; Amiri, R.; Sharifi M.: Comparison of hybrid and ANN methods for estimation of SWE in Samsami sub-watershed. In: Third Water Resources Management Conference, pp. 1–6 (2008)
2. Mashayekhi, D.: The use of snow hydrology for water resources. Off. Water Resour. Surf. Water Sect. (2011) (**in Persian**)
3. Mahmodian, A.H.; Ghasemi, Gh.; Fini, H.; Sarmadi, M.: Shemiran Township, 3rd edn. Iranian Encyclopedia Foundation Press, New York (2009)
4. Nasri, M.; Modarres, R.; Dastorani, M.T.: Application of artificial neural network for runoff estimation case study: Plajan Basin-Zayandehrud watershed. J. Q. Environ. **2**(5), 23–37 (2009)
5. O'Connor, K.: Applied hydrology deterministic. In: Unpublished Lecture Notes. Department of Engineering Hydrology, National University of Ireland, Galway (1997)
6. Chen, J.; Adams, B.J.: Integration of artificial neural networks with conceptual models in rainfall–runoff modeling. J. Hydrol. **318**(1), 232–249 (2006)
7. Duan, D.; Fermini, B.; Nattel, S.: Sustained outward current observed after I (to1) inactivation in rabbit atrial myocytes is a novel Cl-current. Am. J. Physiol.-Heart Circ. Physiol. **263**(6), H1967–H1971 (1992)
8. Sorooshian, S.; Duan, Q.; Gupta, V.K.: Calibration of rainfall–runoff models: application of global optimization to the Sacramento soil moisture accounting model. Water Resour. Res. **29**(4), 1185–1194 (1993)
9. Hsu, K.-l.; Gupta, H.V.; Sorooshian, S.: Artificial neural network modeling of the rainfall–runoff process. Water Resour. Res. **31**(10), 2517–2530 (1995)
10. Wang, W.; Gelder, P.H.V.; Vrijling, J.; Ma, J.: Forecasting daily streamflow using hybrid ANN models. J. Hydrol. **324**(1), 383–399 (2006)
11. Shamseldin, A.Y.: Application of a neural network technique to rainfall–runoff modelling. J. Hydrol. **199**(3), 272–294 (1997)
12. Tokar, A.S.; Johnson, P.A.: Rainfall–runoff modeling using artificial neural networks. J. Hydrol. Eng. **4**(3), 232–239 (1999)
13. Tokar, A.S.; Markus, M.: Precipitation-runoff modeling using artificial neural networks and conceptual models. J. Hydrol. Eng. **5**(2), 156–161 (2000)
14. Bhattacharya, B.; Solomatine, D.: Application of artificial neural network in stage–discharge relationship. In: Proc. 4th International Conference on Hydroinformatics, Iowa City, USA (2000)
15. Dawson, C.; Wilby, R.: Hydrological modelling using artificial neural networks. Prog. Phys. Geogr. **25**(1), 80–108 (2001)
16. Baratti, R.; Cannas, B.; Fanni, A.; Pintus, M.; Sechi, G.M.; Toreno, N.: River flow forecast for reservoir management through neural networks. Neurocomputing **55**(3), 421–437 (2003)
17. Anctil, F.; Rat, A.: Evaluation of neural network streamflow forecasting on 47 watersheds. J. Hydrol. Eng. **10**(1), 85–88 (2005)
18. Matreata, M.: Artificial neural networks and fuzzy logic models in operational hydrological forecasting systems. Geophys. Res. Abstr. 07889 (2006)
19. Nilsson, P.; Uvo, C.B.; Berndtsson, R.: Monthly runoff simulation: comparing and combining conceptual and neural network models. J. Hydrol. **321**(1), 344–363 (2006)
20. Khan, M.S.; Coulibaly, P.: Bayesian neural network for rainfall–runoff modeling. Water Resour. Res. **42**(7) (2006)
21. Baareh, A.K.; Sheta, A.F.; Khnaifes, K.A.: Forecasting river flow in the USA: a comparison between auto-regression and neural network non-parametric models. J. Comput. Sci. **2**(10), 775 (2006)
22. Alvisi, S.; Mascellani, G.; Franchini, M.; Bardossy, A.: Water level forecasting through fuzzy logic and artificial neural network approaches. Hydrol. Earth Syst. Sci. **10**(1), 1–17 (2006)
23. Firat, M.; Güngör, M.: River flow estimation using adaptive neuro fuzzy inference system. Math. Comput. Simul. **75**(3), 87–96 (2007)
24. Aqil, M.; Kita, I.; Yano, A.; Nishiyama, S.: A comparative study of artificial neural networks and neuro-fuzzy in continuous modeling of the daily and hourly behaviour of runoff. J. Hydrol. **337**(1), 22–34 (2007)
25. Banihabib, M.; M. M. a. J. F.: ANN model for investigation of daily correlation among the stations for prediction of input current into Dez dam. Iran. Water Res. J. **4**(7):25–32 (2010)
26. Vafakhah, M.: Application of artificial neural networks and adaptive neuro-fuzzy inference system models to short-term streamflow forecasting. Can. J. Civil Eng. **39**(4), 402–414 (2012)
27. Vafakhah, M.: Comparison of cokriging and adaptive neuro-fuzzy inference system models for suspended sediment load forecasting. Arab. J. Geosci. **6**(8), 3003–3018 (2013)
28. Farahmand, A.S.; Golkar F.; Farahmand, M.V.: Modeling of rainfall–runoff in a river basin using artificial neural network. In: Proceedings of the First Conference of Applied Research of Water Resources. Kermanshah University of Technology, pp. 141–147 (2011)
29. Zare Abyaneh, H.; a. M. B. V.: Evaluation of artificial intelligent and empirical models in estimation of annual runoff. J. Water Soil **25**(2), 365–379 (2011)
30. Kurtulus, B.; Razack, M.: Modeling daily discharge responses of a large karstic aquifer using soft computing methods: artificial neural network and neuro-fuzzy. J. Hydrol. **381**(1), 101–111 (2010)
31. Vafakhah, M.; Mohseni, Saravi M; Mahdavi, M.; Alavipanah, S.K.: Snowmelt runoff prediction by using artificial neural network and adaptive neuro-fuzzy inference system in Taleghan watershed. Iran-Watershed Manage. Sci. Eng. **5**(14), 23–35 (2011)
32. Pustizadeh, N.; Najafi, N.: Discharge prediction by comparing artificial neural network with fuzzy inference system (case study: Zayandehrud River). Iran-Water Resour. Res. **7**(2), 92–97 (2011)
33. Dibike, Y.B.; Velickov, S.; Solomatine, D.; Abbott, M.B.: Model induction with support vector machines: introduction and applications. J. Comput. Civil Eng. **15**(3), 208–216 (2001)
34. Asefa, T.; Kemblowski, M.; McKee, M.; Khalil, A.: Multi-time scale stream flow predictions: the support vector machines approach. J. Hydrol. **318**(1), 7–16 (2006)

35. Yu, P.-S.; Chen, S.-T.; Chang, I.-F.: Support vector regression for real-time flood stage forecasting. J. Hydrol. **328**(3), 704–716 (2006)
36. Behzad, M.; Asghari, K.; Eazi, M.; Palhang, M.: Generalization performance of support vector machines and neural networks in runoff modeling. Expert Syst. Appl. **36**(4), 7624–7629 (2009)
37. Wang, W.-C.; Chau, K.-W.; Cheng, C.-T.; Qiu, L.: A comparison of performance of several artificial intelligence methods for forecasting monthly discharge time series. J. Hydrol. **374**(3), 294–306 (2009)
38. Wu, C.; Chau, K.; Li, Y.: Predicting monthly streamflow using data-driven models coupled with data-preprocessing techniques. Water Resour. Res. **45**(8), W08432 (2009)
39. Moharrampour, M.; Ranjbar, M.K.; Mehrabi, A.: Comparison of support vector machines SVM and statistica in daily flow forecasting. Life Sci. J. **10**(1) (2013)
40. Noori, R.; Khakpour, A.; Omidvar, B.; Farokhnia, A.: Comparison of ANN and principal component analysis-multivariate linear regression models for predicting the river flow based on developed discrepancy ratio statistic. Expert Syst. Appl. **37**(8), 5856–5862 (2010)
41. Okkan, U.; Serbes, Z.A.: Rainfall–runoff modeling using least squares support vector machines. Environmetrics **23**(6), 549–564 (2012)
42. Shahraiyni, H.; Ghafouri, M.; Shouraki, S.; Saghafian, B. Nasseri M.: Comparison between active learning method and support vector machine for runoff modeling. J. Hydrol. Hydromech. **60**(1), 16–32 (2012)
43. Hall, D.K.; Riggs, G.A.; Salomonson, V.V.; Barton, J.; Casey, K.; Chien, J.; DiGirolamo, N.; Klein, A.; Powell, H.; Tait, A.: Algorithm theoretical basis document (ATBD) for the MODIS snow and sea ice-mapping algorithms. NASA GSFC (2001)
44. Hall, D.; Foster, J.; Verbyla, D.; Klein, A.; Benson, C.: Assessment of snow-cover mapping accuracy in a variety of vegetation-cover densities in central Alaska. Remote Sens. Environ. **66**(2), 129–137 (1998)
45. Lee, S.; Ryu, J.-H.; Lee, M.-J.; Won, J.-S.: The application of artificial neural networks to landslide susceptibility mapping at Janghung, Korea. Math. Geol. **38**(2), 199–220 (2006)
46. Coulibaly, P.; Anctil, F.; Bobee, B.: Daily reservoir inflow forecasting using artificial neural networks with stopped training approach. J. Hydrol. **230**(3), 244–257 (2000)
47. Cristianini, N.; Shawe-Taylor, J.: An Introduction to Support Vector Machines and Other Kernel-Based Learning Methods. Cambridge university press, Cambridge (2000)
48. Kecman, V.: Learning and Soft Computing: Support Vector Machines, Neural Networks, and Fuzzy Logic Models. MIT press, Cambridge (2001)
49. Kakaei Lafdani, E.; Moghaddam Nia, A.; Ahmadi, A.: Daily suspended sediment load prediction using artificial neural networks and support vector machines. J. Hydrol. **478**(0), 50–62 (2013)
50. Lorrai, M.; Sechi, G.: Neural nets for modelling rainfall–runoff transformations. Water Resour. Manage. **9**(4), 299–313 (1995)
51. Raghuwanshi, N.; Singh, R.; Reddy, L.: Runoff and sediment yield modeling using artificial neural networks: Upper Siwane River, India. J. Hydrol. Eng. **11**(1), 71–79 (2006)
52. Das, S.K.; Samui, P.; Sabat, A.K.: Prediction of field hydraulic conductivity of clay liners using an artificial neural network and support vector machine. Int. J. Geomech. **12**(5), 606–611 (2011)
53. Muduli, P.K.; Das, M.R.; Samui, P.; Kumar Das, S.: Uplift capacity of suction caisson in clay using artificial intelligence techniques. Mar. Georesour. Geotechnol. **31**(4), 375–390 (2013)